Available online at www.sciencedirect.com

ScienceDirect

C. R. Mecanique 336 (2008) 766–771

Comptes Rendus Mecanique

http://france.elsevier.com/direct/CRAS2B/

Direct sensitivity computation for the Saint-Venant equations with hydraulic jumps

Carole Delenne *, Vincent Guinot, Bernard Cappelaere

Hydrosciences Montpellier, UMR 5569, Université Montpellier 2, place Eugène Bataillon (CCMSE), 34095 Montpellier Cedex 5, France

Received 22 December 2007; accepted after revision 15 September 2008

Available online 11 October 2008

Presented by Olivier Pironneau

Abstract

This Note presents a new Riemann solver for the Saint-Venant equations in conjunction with the sensitivity problem when the solutions are discontinuous. The solver is based on the a priori assumption of two rarefaction waves. The presence of shocks is detected a posteriori and an extra sensitivity term in the form of a Dirac source term is accounted for in the sensitivity balance equations. ***To cite this article: C. Delenne et al., C. R. Mecanique 336 (2008).***

Résumé

Calcul direct de sensibilité pour les équations de Saint-Venant avec ressauts hydrauliques. On propose ici un solveur de Riemann pour résoudre les équations de sensibilité conjointement à la projection sur une dimension des équations de Saint-Venant dans le cas de solutions discontinues. Le solveur est basé sur la supposition a priori de deux ondes de raréfaction. La présence de chocs est détectée a posteriori et un terme supplémentaire, sous la forme d'un terme source de Dirac, est introduit dans l'équilibre des équations de sensibilité. ***Pour citer cet article : C. Delenne et al., C. R. Mecanique 336 (2008).***

Keywords: Computational fluid mechanics; Sensitivity; Hyperbolic conservation laws; Shocks

Mots-clés : Mécanique des fluides numérique ; Sensibilités ; Lois de conservation hyperboliques ; Chocs

Version française abrégée

On cherche à résoudre les équations de sensibilité conjointement à la projection sur une dimension des équations de Saint Venant dans le cas de solutions discontinues. Dans ce cas, en effet, les équations en sensibilité ne peuvent pas être obtenues par une simple dérivation des équations hydrodynamiques de base et un terme source de Dirac apparaît au niveau des chocs. On propose ici une méthode numérique de calcul aux volumes finis, dont le principe est le suivant : (i) définir le problème de Riemann entre deux cellules i et j (issues d'une discrétisation de l'espace)

* Corresponding author.
E-mail addresses: delenne@msem.univ-montp2.fr (C. Delenne), guinot@msem.univ-montp2.fr (V. Guinot), cappelaere@msem.univ-montp2.fr (B. Cappelaere).

1631-0721/$ – see front matter
doi:10.1016/j.crme.2008.09.006

avec des états gauche et droit définis par ces deux cellules respectivement ; (ii) déterminer les valeurs de la variable d'écoulement et/ou des flux dans les régions d'états constants en utilisant les invariants de Riemann, (iii) déterminer les vitesses de propagation des différentes ondes et la localisation de discontinuité par rapport à ces ondes ; (iv) calculer les flux nécessaires pour équilibrer l'équation entre les cellules i et j grâce à la valeur de la variable d'écoulement au niveau de la discontinuité initiale. La solution est alors calculée pour différents pas de temps en utilisant un schéma de discrétisation explicite.

1. The Riemann problem

The Riemann problem of the Saint-Venant and sensitivity equations is first recalled and then the application of the proposed solver is detailed.

The one-dimensional projection of the Saint-Venant equations is a 3×3 Hyperbolic System of Conservation Laws (HSCL), which can be written in vector form as:

$$\left.\begin{aligned} &\frac{\partial \mathbf{U}}{\partial t} + \frac{\partial \mathbf{F}(\mathbf{U}, \phi)}{\partial x} = 0 \\ &\mathbf{U}(x, 0) = \mathbf{U}_0(x, \phi) \\ &\mathbf{U}(x_b, t) = \mathbf{U}_b(t, \phi) \end{aligned}\right\} \quad \text{with } \mathbf{U} = \begin{pmatrix} h \\ q \\ r \end{pmatrix}, \quad \mathbf{F} = \begin{pmatrix} q \\ q^2/h + gh^2/2 \\ qr/h \end{pmatrix} \tag{1}$$

with $\mathbf{U}$: the conserved variable; $\mathbf{F}$: the flux function; ϕ: a parameter on which the flux depends; g: the gravitational acceleration; h: the water depth; q (resp. r): the unit discharge in the x (resp. y) direction; $u = q/h$ (resp. $v = r/h$): the flow velocity in the x (resp. y) direction. The subscripts b and 0 indicate the domain boundary abscissa and the initial condition respectively.

Differentiating the governing equation (1) with respect to the parameter ϕ leads to the equation for the sensitivity $\mathbf{s} = (\eta, \theta, \rho)$ of $\mathbf{U}$ to ϕ:

$$\frac{\partial \mathbf{s}}{\partial t} + \frac{\partial}{\partial x}(\mathbf{A}\mathbf{s}) = -\frac{\partial}{\partial x}\left(\frac{\partial \mathbf{F}}{\partial \phi}\right) \tag{2}$$

with $\mathbf{A} = \partial \mathbf{F}/\partial \mathbf{U}$.

However, this derivation is correct only under the assumption of a continuous and differentiable solution $\mathbf{U}$ [1]. In the presence of a discontinuity, the so-called Rankin–Hugoniot conditions (or jump relationships) must be used:

$$\mathbf{F}_\mathrm{L} - \mathbf{F}_\mathrm{R} = (\mathbf{U}_\mathrm{L} - \mathbf{U}_\mathrm{R})c_s$$

where c_s is the discontinuity speed, and where the index L and R denote the left and right states across the discontinuity. Moreover, since $\mathbf{U}$ and $\mathbf{s}$ are independent variables, the sensitivities $\mathbf{s}_\mathrm{L}$ and $\mathbf{s}_\mathrm{R}$ on the left and right-hand side of the discontinuity are independent from $\mathbf{U}_\mathrm{L}$ and $\mathbf{U}_\mathrm{R}$. Consequently, the jump relationship for the sensitivity is much more complex than that for the flow variable [2,3] and implies a specific source term $\mathbf{R}$, in a form of a Dirac function, which takes effect only at the discontinuity:

$$\mathbf{H}_\mathrm{L} - \mathbf{H}_\mathrm{R} + \mathbf{R} = (\mathbf{s}_\mathrm{L} - \mathbf{s}_\mathrm{R})c_s$$

with $\mathbf{s}$ the conserved variable and $\mathbf{H} = \mathbf{A}\mathbf{s}$ the flux function for sensitivity. Then,

$$\mathbf{R} = (\mathbf{s}_\mathrm{L} - \mathbf{s}_\mathrm{R})c_s - \mathbf{H}_\mathrm{L} + \mathbf{H}_\mathrm{R} = (\mathbf{A}_\mathrm{R} - c_s\mathbf{I})\mathbf{s}_\mathrm{R} - (\mathbf{A}_\mathrm{L} - c_s\mathbf{I})\mathbf{s}_\mathrm{L}$$

which can be written as:

$$\mathbf{R} = \Delta\big[(\mathbf{A} - c_s\mathbf{I})\mathbf{s}\big] \tag{3}$$

The source term $\mathbf{R}$ is non-zero only when there is a shock. Indeed, when the discontinuity is a contact one, c_s is an eigenvalue of the matrix $\mathbf{A}$ and $(\mathbf{A}_{\mathrm{R,L}} - c_s\mathbf{I}) = 0$.

Because this Jacobian matrix **A** depends on the solution **U**, the Riemann problem of the sensitivity cannot be considered independently from the one of the flow variable. We thus consider the following initial-value problem:

$$\left.\begin{aligned}&\frac{\partial \mathbf{U}}{\partial t}+\frac{\partial \mathbf{F}}{\partial x}=0\\&\frac{\partial \mathbf{s}}{\partial t}+\frac{\partial \mathbf{H}}{\partial x}=\Delta\big[(\mathbf{A}-c_s\mathbf{I})\mathbf{s}\big]\\&(\mathbf{U},\mathbf{s})(x,0)=\begin{cases}(\mathbf{U}_\mathrm{L},\mathbf{s}_\mathrm{L}) & \text{for } x<0\\(\mathbf{U}_\mathrm{R},\mathbf{s}_\mathrm{R}) & \text{for } x>0\end{cases}\end{aligned}\right\}\tag{4}$$

which is a 3×3 HSCL with the following eigenvalues:

$$\big(\lambda^{(1)},\lambda^{(2)},\lambda^{(3)}\big)=(u-c,u,u+c)\tag{5}$$

The general solution of the Riemann problem is made of three waves separating two internal regions of constant state. In the exact solution of the Riemann problem, the second wave (with celerity $\lambda^{(2)}=u$) is a contact discontinuity, while the first and third waves may be of any type, depending on $\mathbf{U}_\mathrm{L}$ and $\mathbf{U}_\mathrm{R}$. Although not strictly valid across a shock, the Riemann invariants may be used to approximate the jump relationships (e.g. [4–8]). Then, the nature of the waves in the Riemann problem may be guessed a priori without a posteriori verification and the resulting system of algebraic equations may be solved to determine directly the solution in the intermediate regions of constant state. The proposed approximate-state Riemann solver uses the assumption that the eigenvalues (5) are the celerities of three rarefaction waves. In what follows, we assess the sensitivity of the solution to the initial value of the left or right state of **U**.

2. The approximate-state Riemann solver

2.1. Discretization

The solution will be advanced in time using the following discretization of (4):

$$\mathbf{U}_i^{n+1}=\mathbf{U}_i^n+\frac{\Delta t}{\Delta x_i}\big(\mathbf{F}_{i-\frac{1}{2}}^{n+\frac{1}{2}}-\mathbf{F}_{i+\frac{1}{2}}^{n+\frac{1}{2}}\big)\tag{6}$$

$$\mathbf{s}_i^{n+1}=\mathbf{s}_i^n+\frac{\Delta t}{\Delta x_i}\big(\mathbf{H}_{i-\frac{1}{2}}^{n+\frac{1}{2}}-\mathbf{H}_{i+\frac{1}{2}}^{n+\frac{1}{2}}+\mathbf{R}_{i-\frac{1}{2},i}^{n+\frac{1}{2}}+\mathbf{R}_{i+\frac{1}{2},i}^{n+\frac{1}{2}}\big)\tag{7}$$

where $\mathbf{U}_i^n$ and $\mathbf{s}_i^n$ are the average values of **U** and **s** over the cell i at the time n; $\mathbf{F}_{i-\frac{1}{2}}^{n+\frac{1}{2}}$ and $\mathbf{H}_{i-\frac{1}{2}}^{n+\frac{1}{2}}$ are the average values of the fluxes **F** and **H** at the interface $i-\frac{1}{2}$ between the cells $i-1$ and i over the time interval $[t^n,t^{n+1}]$; $\mathbf{R}_{i-\frac{1}{2},i}^{n+\frac{1}{2}}$ and $\mathbf{R}_{i+\frac{1}{2},i}^{n+\frac{1}{2}}$ represent the contributions of the source terms possibly generated by shocks propagating respectively from the interfaces $i+\frac{1}{2}$ and $i-\frac{1}{2}$ into the cell i; Δt is the computational time step and Δx_i is the width of the cell i.

For each interface between two cells i and j (issued from a spatial discretization), a Riemann problem is defined with left and right states taken from these cells. Then, the proposed solver uses the classical HLL approach to compute the solution in the continuous case and a specific treatment of the shocks.

2.2. Continuous case

The Riemann invariants for (4) are defined as [9]:

$$\begin{cases}\mathrm{d}(u-2c)=0 & \text{for } \dfrac{\mathrm{d}x}{\mathrm{d}t}=u-c\\[2mm]\mathrm{d}v=0 & \text{for } \dfrac{\mathrm{d}x}{\mathrm{d}t}=u\\[2mm]\mathrm{d}(u+2c)=0 & \text{for } \dfrac{\mathrm{d}x}{\mathrm{d}t}=u+c\end{cases}\tag{8}$$

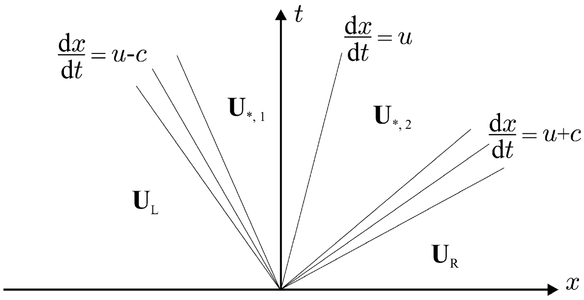

Fig. 1. Scheme of the different regions for the Saint-Venant equations solution

and therefore, noting χ, ν, ω the sensitivities of c, u, v with respect to the parameter ϕ:

$$\begin{cases} \mathrm{d}(\nu - 2\chi) = 0 & \text{for } \dfrac{\mathrm{d}x}{\mathrm{d}t} = u - c \\ \mathrm{d}\omega = 0 & \text{for } \dfrac{\mathrm{d}x}{\mathrm{d}t} = u \\ \mathrm{d}(\nu + 2\chi) = 0 & \text{for } \dfrac{\mathrm{d}x}{\mathrm{d}t} = u + c \end{cases} \tag{9}$$

In the regions of constant state (see Fig. 1), using the approximate expressions (8) and (9) yields:

$$\begin{cases} c_{*,1} = c_{*,2} = \frac{1}{2}(c_\mathrm{L} + c_\mathrm{R}) + \frac{1}{4}(u_\mathrm{L} - u_\mathrm{R}) \\ u_{*,1} = u_{*,2} = \frac{1}{2}(u_\mathrm{L} + u_\mathrm{R}) + c_\mathrm{L} - c_\mathrm{R} \\ v_{*,1} = v_\mathrm{L} \\ v_{*,2} = v_\mathrm{R} \end{cases} \tag{10}$$

$$\begin{cases} \chi_{*,1} = \chi_{*,2} = \frac{1}{2}(\chi_\mathrm{L} + \chi_\mathrm{R}) + \frac{1}{4}(\nu_\mathrm{L} - \nu_\mathrm{R}) \\ \nu_{*,1} = \nu_{*,2} = \frac{1}{2}(\nu_\mathrm{L} + \nu_\mathrm{R}) + \chi_\mathrm{L} - \chi_\mathrm{R} \\ \omega_{*,1} = \omega_\mathrm{L} \\ \omega_{*,2} = \omega_\mathrm{R} \end{cases} \tag{11}$$

where the subscript *,1 and *,2 denote the values of the variables in the intermediate regions of constant state on the left and right-hand sides of the contact discontinuity, respectively. The flux **H** in the regions of constant state is then determined uniquely from (11):

$$\mathbf{H}_{*,p} = \begin{bmatrix} \theta_{*,p} \\ (c_{*,p}^2 - u_{*,p}^2)\eta_{*,p} + 2u_{*,p}\theta_{*,p} \\ -u_{*,p}v_{*,p}\eta_{*,p} + v_{*,p}\theta_{*,p} + u_{*,p}\rho_{*,p} \end{bmatrix}, \quad p = 1, 2$$

Using the fact that $h = c^2/g$, $q = hu$ and $r = hv$, yields the sensitivity $\mathbf{s}_{*,p}$:

$$\begin{pmatrix} \eta \\ \theta \\ \rho \end{pmatrix}_{*,p} = \begin{pmatrix} 2c\chi/g \\ \eta u + h\nu \\ \eta v + h\omega \end{pmatrix}_{*,p}$$

2.3. *Shock treatment*

A shock appears on the first or third wave when either $u_\mathrm{L} - c_\mathrm{L} > u_\mathrm{R} - c_\mathrm{R}$ or $u_\mathrm{L} + c_\mathrm{L} > u_\mathrm{R} + c_\mathrm{R}$. The source term **R** is zero everywhere except at the interfaces where a shock is detected. The shock speed is estimated using one of the following relationships (with the superscript L and 1 or R and 2 if the shock is on the first or third wave respectively):

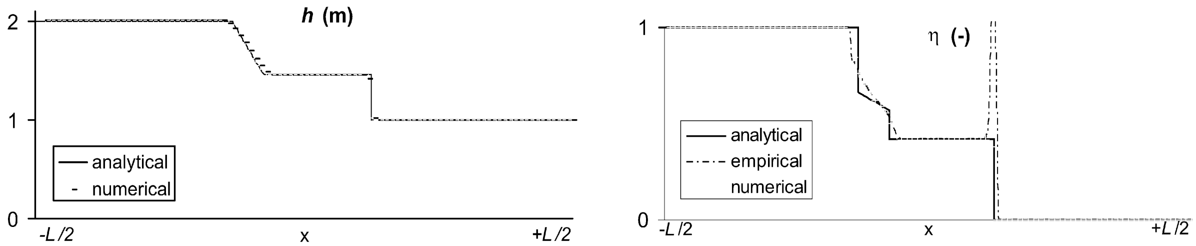

Fig. 2. Water height h and sensitivity η to the initial left water height value h_{L}. The numerical and analytical solutions are shown, as well as the empirical computation of the sensitivity.

$$c_s = \frac{q_{\{\mathrm{L,R}\}} - q_{*,\{1,2\}}}{h_{\{\mathrm{L,R}\}} - h_{*,\{1,2\}}}$$
$$c_s = \frac{(q^2/h + gh^2/2)_{\{\mathrm{L,R}\}} - (q^2/h + gh^2/2)_{*,\{1,2\}}}{q_{\{\mathrm{L,R}\}} - q_{*,\{1,2\}}}$$

or $(u_{\{\mathrm{L,R}\}} + u_{*,\{1,2\}})/2$ if the previous two denominators are null.

If the shock speed in negative, the corresponding wave travels from the interface $i - \frac{1}{2}$ into the cell $i - 1$ and does not yield any source term in the cell i. In contrast, if the speed is positive, the wave travels into the cell i and contributes to the source term $\mathbf{R}^{n+\frac{1}{2}}_{i-\frac{1}{2},i}$ by a quantity given by Eq. (3).

This shock treatment cannot be considered as a shock tracking procedure in the classical sense in that the exact location of the discontinuity within the cell does not need to be known.

2.4. Fluxes at the interface

At the end of the process, the fluxes can be computed at the interface using:

$$\mathbf{F}^{n+\frac{1}{2}}_{i-\frac{1}{2}} = \mathbf{F}\big(\mathbf{U}^{n+\frac{1}{2}}_{i-\frac{1}{2}}\big)$$
$$\mathbf{A}^{n+\frac{1}{2}}_{i-\frac{1}{2}} = \mathbf{A}\big(\mathbf{U}^{n+\frac{1}{2}}_{i-\frac{1}{2}}\big)$$
$$\mathbf{H}^{n+\frac{1}{2}}_{i-\frac{1}{2}} = \mathbf{A}^{n+\frac{1}{2}}_{i-\frac{1}{2}}\mathbf{s}^{n+\frac{1}{2}}_{i-\frac{1}{2}}$$

The whole process is then repeated in time using Eqs. (6) and (7).

2.5. Examples

Fig. 2 shows the water depth and depths sensitivity profile computed using the proposed algorithm for the classical dam-break problem. The sensitivity to the water level on the left-hand side of the dam is computed, therefore $\eta_{\mathrm{L}} = 1$ and $\eta_{\mathrm{R}} = 0$. Fig. 2 also shows the empirical sensitivity profile, computed from the difference between two simulations carried out using slightly different values for the water depth h_{L} on the left-hand side of the dam. As shown in Fig. 2, the empirical sensitivity profile exhibits an artificial peak across the shock. The peak in the empirical sensitivity is due to the fact that the propagation speed of the shock (and therefore its location) is a function of the water depth h_{L}. A small variation in h_{L} induces a shift in the location of the shock, and consequently a large depth variation in the cells in which the shock is located. Dividing this variation by the small variation in h_{L} leads to an artificially large sensitivity. Paradoxically, using a smaller difference in h_{L} does not lead to numerical convergence and yields a higher artificial peak value. As shown in the computational results, accounting for the Dirac source term $\mathbf{R}$ in Eq. (7) allows the artificial peak to be eliminated from the simulation.

Fig. 3 shows the water depth and sensitivity profiles computed for an initial state formed by the superimposition of two dam-break problems. The initial water depth is piecewise constant in three subregions of the computational domain. The three water stages decrease from left to right. Although no analytical solution is known for such initial

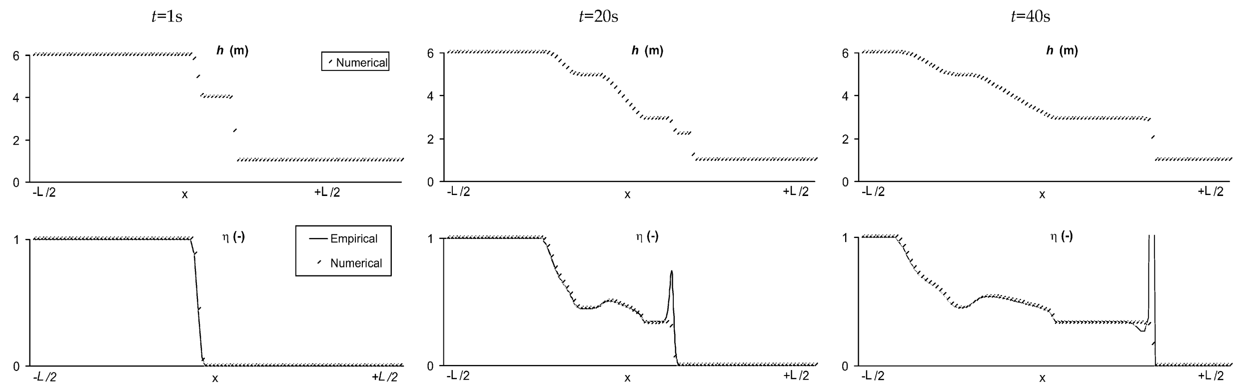

Fig. 3. Successive calculations of water height h and sensitivity η to the initial left water height value h_L in case of two shocks.

conditions, the solution is known to be made of two rarefaction waves heading to the left and two shocks heading to the right. The shocks traveling to the right eventually merge into a single one, as shown in Fig. 3. The empirical sensitivity profile exhibits an artificial peak in the neighborhood of the faster shock, while the sensitivity profile computed using the proposed algorithm does not. This is another indication that the Dirac source term **R** is estimated accurately in this case.

Conclusion

The proposed approximate state Riemann solver has been applied here to solve the shallow water and sensitivity equations when one or several shocks are present in the solution. It will be generalized to other HSCL and other case studies in forthcoming publications.

References

[1] M.D. Gunzburger, Sensitivities, adjoints and flow optimization, Int. J. Numer. Methods Fluids 31 (1999) 53–78.
[2] C. Bardos, O. Pironneau, A formalism for the differentiation of conservation laws, C. R. Acad. Sci. Paris, Ser. I 335 (2002) 839–845.
[3] V. Guinot, M. Leménager, B. Cappelaere, Sensitivity equations for hyperbolic conservation law-based flow models, Adv. Water Resour. 30 (2007) 1943–1961.
[4] P.D. Lax, Hyperbolic systems of conservation laws, Comm. Pure Appl. Math. 10 (1957) 537–566.
[5] E.F. Toro, Riemann Solvers and Numerical Methods for Fluid Dynamics, Springer, 1997.
[6] V. Guinot, Godunov-type Schemes. An Introduction for Engineers, Elsevier, 2003.
[7] V. Guinot, Riemann solvers for water hammer simulations by Godunov method, Int. J. Numer. Methods Engrg. 49 (2000) 851–870.
[8] J. Lhomme, V. Guinot, A general, approximate-state Riemann solver for hyperbolic systems of conservation laws with source terms, Int. J. Numer. Methods Fluids 56 (2007) 1605–1623.
[9] V. Guinot, Ondes en mécanique des fluides. Modélisation et simulation numérique, Hermes Publishing, 2006 (in French).